Early Triassic Stuhini Group and Tertiary Sloko Group Magmatism (NTS 104K/10W), Northwestern British Columbia: New U-Pb Geochronological Results

by A.T. Simmons[1], R.M. Tosdal[1], H.J. Awmack[2], J.L. Wooden[3] and R.M. Friedman[1]

INTRODUCTION

Upper Triassic volcanism represented by the Stuhini and Takla-Nicola groups is a major component of the Stikine and Quesnel terranes of the Canadian Cordillera. These two groups represent important arc-building products and host many of British Columbia's ore deposits. Despite their importance, the timing of volcanism and basic knowledge of their environment of formation remain poorly constrained. To date, there is only one known U-Pb age of 212.8 +4.2/–3.5 Ma (Logan *et al.*, 2000) from a rhyolitic unit within the Stuhini Group in the Iskut River area. Additionally, subvolcanic Stuhini Group intrusions have yielded U-Pb zircon ages of 216.7 ±4 Ma and 214 ±1 Ma from leucogabbro intrusions in northern British Columbia (Hart, 1995; Mihalynuk *et al.*, 1997). Other K-Ar ages have been reported, but these represent minimum ages (*e.g.*, Logan *et al.*, 2000).

In 2003, a research project initiated by the Mineral Deposit Research Unit (MDRU) at the University of British Columbia (UBC) investigated Late Cretaceous volcanoplutonic complexes in the Taku River area of the Stikine Terrane, northwestern British Columbia (Fig 1). A critical component of the study was also the Upper Triassic Stuhini Group and Lower to Middle Jurassic Laberge Group rocks, which are the country/hostrocks of these volcanoplutonic complexes. Work reported herein is drawn from fieldwork spanning 2003 through 2005 and from Simmons (2005). Funding for the project was derived in part from the Rocks to Riches Program, which was administered by the BC and Yukon Chamber of Mines (now the Association for Mineral Exploration BC) and from the Natural Sciences and Engineering Research Counsel of Canada (NSERC) though an Industrial Post-Graduate Fellowship and a Discovery Grant, the Society of Economic Geologists, Equity Engineering Ltd., Rimfire Minerals Corporation and Cangold Limited.

During fieldwork from 2003 to 2005, approximately nine weeks of mapping and sampling were carried out over an area extending from the Bing prospect in the southeast to Mount Lester Jones in the northeast (Fig 2). Although the
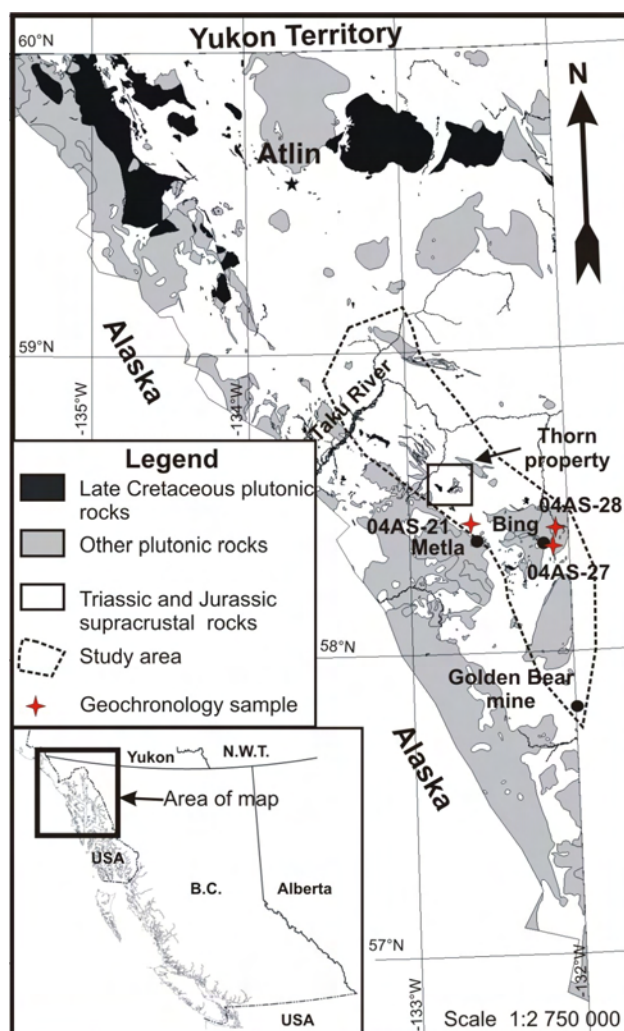

Figure 1. Location of 2003–2005 fieldwork, showing the distribution of pre-Cretaceous, Cretaceous and post-Cretaceous rocks. Additionally, locations of geochronology and geochemistry samples reported herein are given for data south of the Thorn property. Locations of mineral exploration prospects are shown for reference.

[1] *Mineral Deposit Research Unit, Department of Earth and Ocean Sciences, University of British Columbia, Vancouver, BC*

[2] *Equity Engineering Ltd, Vancouver, BC*

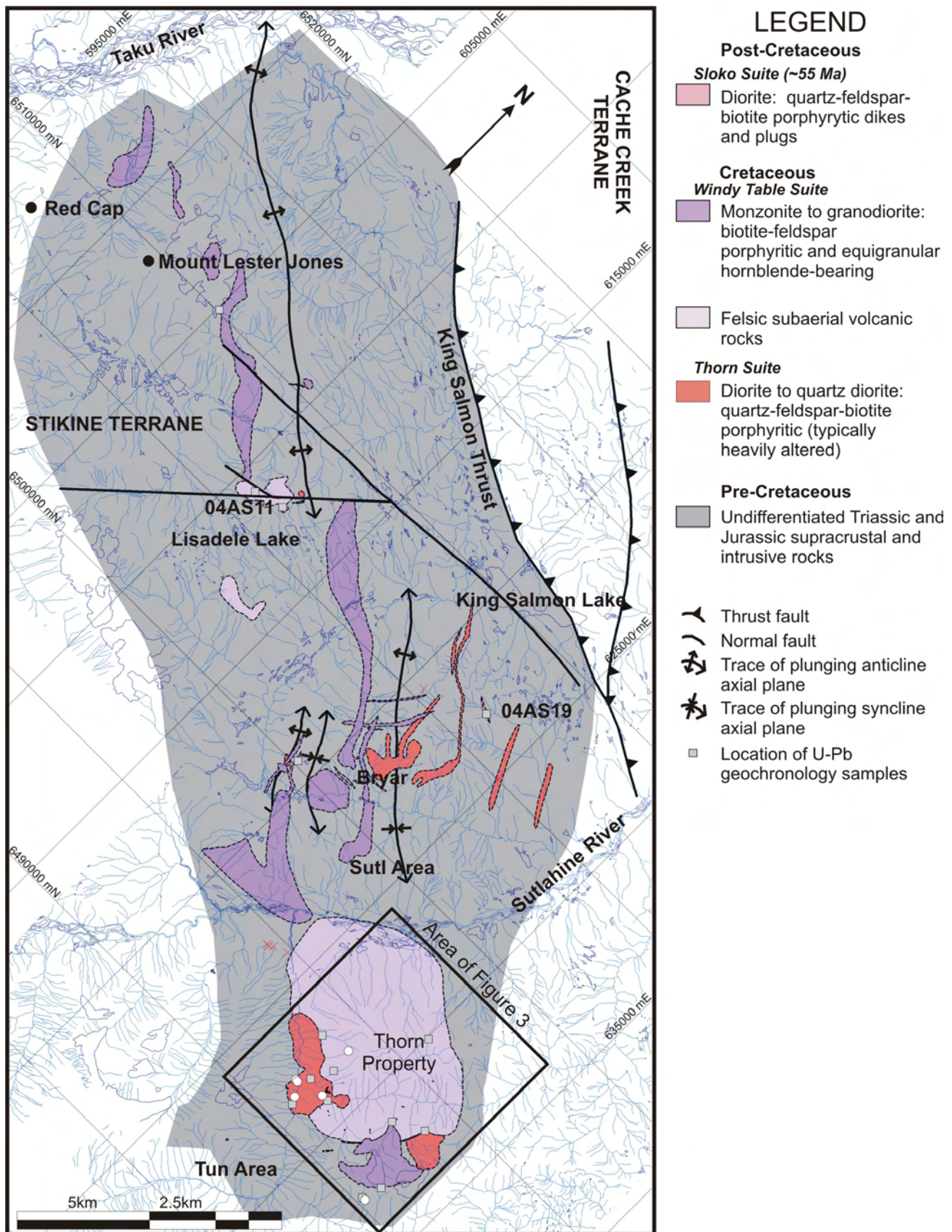[3] *United States Geological Survey, Menlo Park, CA*

Figure 2. Regional geology of the study area, highlighting postaccretionary magmatic rocks with geochronology and geochemistry sample locations for data north of the Thorn property.

focus was mainly on Late Cretaceous rocks, significant effort was devoted to the relative timing of all rock types, including Stuhini Group, Sloko Group and other non-Cretaceous plutonic rocks, and the collection of samples suitably constrained for absolute timing using U-Pb methods on zircon. Geochronology was performed using both sensitive high (mass)-resolution ion microprobe – reverse geometry (SHRIMP-RG) and isotope dilution – thermal ionization mass spectrometry (ID-TIMS) at Stanford University and the University of British Columbia, respectively. Geochronological results for non-Cretaceous rocks are presented herein. Cretaceous geology and geochronology will be presented in future publications.

REGIONAL GEOLOGICAL CONTEXT

The Stikine, Cache Creek and Quesnel tectonostratigraphic terranes underlie the region, with Stikinia being the host terrane in the study area (Fig 1). The evolution of these terranes is a topic of much debate, with several different models currently existing; however, the model of Mihalynuk *et al.* (1994) is favoured here due to the proximity of this study to where the model was developed, which accounts for particular rock types present in the northern Cordillera. These terranes represent a continuous approximately 1400 km long island arc formed outboard of western ancestral North America along a northwest-trending subduction zone during and prior to the Late Carboniferous (Mihalynuk *et al.*, 1994). A Late Permian to Late Triassic reconfiguration of the subduction zone followed the initial stage of collapse of the Slide Mountain Basin during east-verging contraction (Nelson, 1993). The subduction zone was re-established outboard of Quesnellia and Stikinia by the Late Triassic, and the magmatic products are represented by the Stuhini and Nicola-Takla groups. Oroclinal bending of the terranes was also initiated during this time, in response to the collision of the Cache Creek plateau with Quesnellia and Stikinia (Mihalynuk *et al.*, 1994).

Extensive arc volcanism and plutonism dominated Stikinia and Quesnellia in the Late Triassic. Generally, the Triassic volcanic rock sequences are very similar, grading from subalkaline volcanic rocks (Stuhini and Nicola-Takla Groups, respectively) in the south to volcaniclastic sedimentary rocks (Lewes River Group and Nazcha Formation, respectively) in the north (Gabrielse, 1969). Arc-derived sedimentary rocks dominate the Late Triassic arc near the proposed oroclinal hinge, whereas arc volcanic rocks dominate elsewhere along the arc (Gabrielse, 1969). Monger *et al.* (1991) and Jackson (1992) provided evidence for the linkage of the Stikinia and Cache Creek terranes at this time, while the linkage between Cache Creek and Quesnellia (albeit in southern British Columbia) was provided by Monger (1984).

Clastic sedimentary rocks of the Lower to Middle Jurassic Laberge Group were deposited unconformably on the Late Triassic Stuhini Group throughout the region. Mihalynuk (1999) proposed that these sedimentary rocks recorded dissection of the Stuhini arc at the hinge zone of the oroclinal bend. South of the hinge zone, continued subduction under Stikinia and Quesnellia resulted in voluminous calcalkaline Hazelton Group volcanism. Nixon *et al.* (1993) established that Quesnellia was emplaced against the western margin of North America by 186 Ma. Locally, clastic sedimentary rocks are composed of detritus from older Laberge Group strata, indicating that rapid up-

lift occurred in limited areas. This basin cannibalization may represent the initial collapse leading to the Whitehorse Trough (Mihalynuk, 1999). Southwest-verging thrust faults play an important role in the development of the arc at this time. For example, the southwest-verging movement of the King Salmon thrust (Thorstad and Gabrielse, 1986) allowed for the emplacement of the Laberge Group and the formation of the clastic foredeep of the proto–Bowser Basin, which began in latest Toarcian to Aalenian time (Ricketts *et al.*, 1992; Mihalynuk, 1999).

Prior to the Middle Jurassic, the Stikine, Quesnel and Cache Creek terranes were discrete tectonic elements separated by subduction or collision zones. In the Middle Jurassic, Quesnellia was thrust over western North America, and the Cache Creek was thrust over Stikinia. Mihalynuk (1999) estimated shortening in excess of 50% in the Tagish Lake vicinity, approximately 100 km north of the study area. There, the Cache Creek and Stikine terranes were stitched together by 172 Ma by the undeformed Fourth of July batholith (Mihalynuk and Smith, 1992). Sedimentation in the Laberge Basin ceased by the latest Middle Jurassic and a period of tectonic quiescence followed, marking the beginning of a magmatic lull that lasted some 50 m.y.

By the Cretaceous, magmatism and strike-slip deformation dominated the tectonics of the northern Cordillera. Magmatism resumed in the latest Early Cretaceous with the onset of the Whitehorse Magmatic Epoch, which lasted from approximately 111 Ma (Hart, 1995) until 100 Ma (Mihalynuk, 1999). A series of felsic pyroclastic rocks and igneous intrusions, emplaced episodically during the Late Cretaceous, can be separated into two distinct periods: the Thorn suite (93–88 Ma) and Windy Table suite (86–80 Ma; Simmons *et al.*, 2005; Simmons, 2005).

Following another magmatic hiatus, magmatism resumed from 59 to 53 Ma (Mihalynuk, 1999) as part of the Sloko suite. These intermediate to felsic magmatic rocks are represented by voluminous eruptions of volcanic rocks with coeval semicircular granitic plutons, which mark the roots of Sloko-age volcanoes in the Coast Belt (Mihalynuk, 1999). Swarms of north-northeast to north-northwest-trending porphyritic quartz diorite dikes may have fed Sloko volcanic rocks.

GEOCHRONOLOGY METHODS

U-Pb Isotope Dilution Thermal Ionization Mass Spectrometry (ID-TIMS)

Zircon was separated from rock samples using conventional crushing, grinding and Wilfley table techniques, followed by final concentration using heavy liquids and magnetic separations. Mineral fractions for analysis were selected based on grain morphology, quality, size and magnetic susceptibility. All zircon fractions were air abraded prior to dissolution to minimize the effects of postcrystallization Pb loss, using the technique of Krogh (1982). All mineral separations, geochemical separations and mass spectrometry were done at the Pacific Centre for Isotopic and Geochemical Research in the Department of Earth and Ocean Sciences, University of British Columbia. Samples were dissolved in concentrated HF and HNO_3 in the presence of a mixed $^{233-235}U$-^{205}Pb tracer. Separation and purification of Pb and U employed ion exchange column techniques modified slightly from those described by

Parrish *et al.* (1987). The Pb and U were eluted separately and loaded together on a single Re filament using a phosphoric acid – silica gel emitter. Isotopic ratios were measured using a modified single-collector VG-54R thermal ionization mass spectrometer equipped with a Daly photomultiplier. Measurements were done in peak-switching mode on the Daly detector. Analytical blanks for U and Pb were in the range 1 pg and 1 to 5 pg, respectively, during the course of this study. Fractionation of U was determined directly on individual runs using the $^{233-235}$U tracer, and Pb isotopic ratios were corrected for a fractionation of 0.37%/amu for Faraday and Daly runs, respectively, based on replicate analyses of the NBS-981 Pb standard and the values recommended by Thirlwall (2000). All analytical errors were numerically propagated through the entire age calculation using the technique of Roddick (1987). Concordia intercept ages and associated errors were calculated using a modified version the York-II regression model (wherein the York-II errors are multiplied by the mean standard weighted deviate [MSWD]) and the algorithm of Ludwig (1980).

U-Pb Sensitive High-Resolution Ion Microprobe – Reverse Geometry (SHRIMP-RG) Zircon Geochronology

The samples were prepared at the University of British Columbia using the methods outlined for U-Pb TIMS analysis. The populations of zircons obtained from these samples were dated using the SHRIMP-RG at Stanford University, California. The SHRIMP-RG has a reverse geometry design and has improved mass resolution compared to conventional SHRIMP designs (Williams, 1998; Bacon *et al.*, 2000). Bacon *et al.* (2000) summarized the operational conditions for the SHRIMP-RG. Reviews on the ion microprobe technique and data interpretation are provided in Ireland and Williams (2003). Initial common Pb compositions were based on the measured ^{204}Pb and the model of Cumming and Richards (1975). Zircon and Pb isotope data were reduced using the SQUID (Ludwig, 2001) and Isoplot programs (Ludwig, 1999, 2003).

FIELD MAPPING STUDIES IN THE TAKU RIVER AREA

The study area is located on the western margin of the Stikine tectonostratigraphic terrane, where the Coast Belt meets the Intermontane Belt, as defined by Wheeler and McFeely (1987). Three distinct periods of magmatism postdate the amalgamation of Stikinia, Cache Creek and Quesnellia, and their accretion onto the western flank of North America. These magmatic bodies were emplaced into and deposited onto Upper Triassic subaqueous mafic

volcanic rocks and associated marine sedimentary rocks (Stuhini Group) and Lower to Middle Jurassic clastic sedimentary rocks (Laberge Group). Stuhini Group rocks are the oldest rocks mapped in the study area and are unconformably overlain by the Laberge Group at a shallow angle, east of the Outlaw zone on the Thorn property (Simmons *et al.*, 2005). The basement rocks were deformed during the amalgamation of Stikinia, Cache Creek and Quesnellia, and their subsequent accretion onto the western flank of North America. Deformation during this period is characterized by regional sub-greenschist metamorphism; northwest-trending, upright, open to closed folds; and northwest-trending trust faults. The plutonic rocks of the Fourth of July suite intruded the basement rocks by 168 Ma and cut deformed Mesozoic rocks, indicating that amalgamation and accretion had ceased prior to these intrusions. North of the project area, in the Tagish Lake vicinity, Mihalynuk (1999) demonstrated that *ca.* 172 Ma plutons of the Fourth of July suite cut deformed Mesozoic rocks. Eocene Sloko suite magmatism is recognized in two locales within the study area, the Lisadele Lake and King Salmon Lake areas, as plagioclase-biotite-porphyritic dikes.

Late Cretaceous intrusive and volcanic rocks of the Thorn and Windy Table suites will be described in more detail elsewhere (A.T. Simmons *et al.*, work in progress).

A summary of the geochronology presented herein is given in Table 1.

Stuhini Group

Strata of the Stuhini Group form a northwesterly-trending belt that extends through the entire study area from the vicinity of the Golden Bear mine to the Tulsequah area, where the rocks were named by Kerr (1948) after Stuhini Creek. These strata continue to the north through the Tagish Lake area (Mihalynuk, 1999) and are correlative with the Lewis River Group farther north (Wheeler, 1961; Hart *et al.*, 1989).

A wide range of rock types, including basic to intermediate subalkaline flows, pyroclastic rocks and related sedimentary rocks, characterize the Stuhini Group (Mihalynuk, 1999). The group is divided in the study area into a sequence dominated by submarine volcanic rocks and one dominated by clastic sedimentary rocks and lesser carbonate rocks. Near the Thorn property (Fig 3), submarine mafic volcanic strata are overlain by sedimentary strata (Baker, 2003; Simmons *et al.*, 2005) and are similar to the section described by Mihalynuk (1999) at Willison Bay, approximately 90 km north of the study area.

On the Thorn property, the Stuhini Group consists of submarine mafic volcanic rocks at the base, changing up the stratigraphic section to include increasing amounts of intercalated siltstone and conglomerate. South of the Thorn

TABLE 1. SUMMARY OF GEOCHRONOLOGY RESULTS PRESENTED IN THE PAPER.

Sample	UTM Zone 8 (NAD 83)		Method	Age (Ma)	Error (Ma) at 1 level	Sample description
	Easting[1]	Northing[1]				
04AS-21	636336	6479072	SHRIMP-RG U-Pb zircon	249.0	±6.4	Stuhini Group andesitic lapilli and crystal tuff
04AS-27	667318	6472437	SHRIMP-RG U-Pb zircon	214.2	±2.4	Stuhini Group subvolcanic intrusion-foliated gabbro
04AS-28	668843	6479202	SHRIMP-RG U-Pb zircon	219.2	±2.4	Stuhini Group subvolcanic granodiorite intrusion
AS-071a	632543	6490270	ID-TIMS U-Pb zircon	168.1	±0.7	Fourth of July suite rhyodacite dike
04AS-11	612037	6506538	SHRIMP-RG U-Pb zircon	56.3	±0.7	Sloko suite diorite porphyry
04AS-19	622970	6506461	SHRIMP-RG U-Pb zircon	55.5	±0.6	Sloko suite diorite porphyry

Explanation

Stratified Rocks
Windy Table Suite

Phase 3: Dacitic lapilli and crystal tuff. Variable welding, grain size and fragment types throughout. Welding most dense near base and middle Phase 3 strata. Base of deposit dominantly ash, with lapill-size fragments increasing upwards. Clast types include pumice, foreign wallrock, plant debris and flow-foliated rhyolite of Phase 2.

Phase 2: Fine-grained, rhyolitic, quartz-feldspar-biotite-phyric, flow-foliated units. Flow foliations defined by quartz and feldspar phenocrysts. Foliation may be intensely folded and, near the centre of the flow domes, foliation may be absent and phenocryst size increases.

Phase 1: Andesitic lapilli tuff with lesser horizons of reworked volcaniclastic sedimentary rocks and dacitic lapilli tuff petrographically similar to Phase 3. Andesitic units contain abundant broken feldspar crystals and rare pumice. Fragments are generally fine lapilli size.

Undifferentiated Windy Table suite rocks.

Pre-Cretaceous Rocks

Undifferentiated Upper Triassic submarine mafic volcanic and associated sedimentary rocks and Lower to Middle Jurassic calcareous clastic sedimentary rocks of the Stuhini and Laberge groups, respectively.

Intrusive Rocks
Windy Table Suite

Type 1: Monzonite to granodiorite; crowded to matrix-supported feldspar, hornblende porphyry. Quartz is generally restricted to the matrix with feldspar, magnetite and lesser titanite and apatite and rare pyroxene.

Type 2: Quartz monzonite to monzogranite granophyric rocks. Appear equigranular in outcrop and contain hornblende, plagioclase and feldspar-quartz intergrowths. Lesser phases include biotite, magnetite and titanite.

Type 4: Rhyolitic, aphanitic, occasionally feldspar-phyric, flow-foliated dikes. Intrude around the periphery of the Thorn volcanic centre and are generally no wider than 3 m.

Thorn Suite

Quartz diorite; crowded quartz-feldspar-biotite porphyry. Contains distinctive coarse-grained rounded quartz phenocrysts and coarse-grained euhedral biotite phenocrysts. Less porphyritic and may be flow-foliated near the margins.

Fourth of July Suite

MJRIN: Rhyodacitic, aphanitic, 3-5 m wide, flow-foliated dykes. Rarely feldspar-phyric.

◆ U-Pb geochronology sample location. Labels in italics from Mihalynuk et al. (2003)

★ Mineralized zone location

╲ Surface trace of normal fault

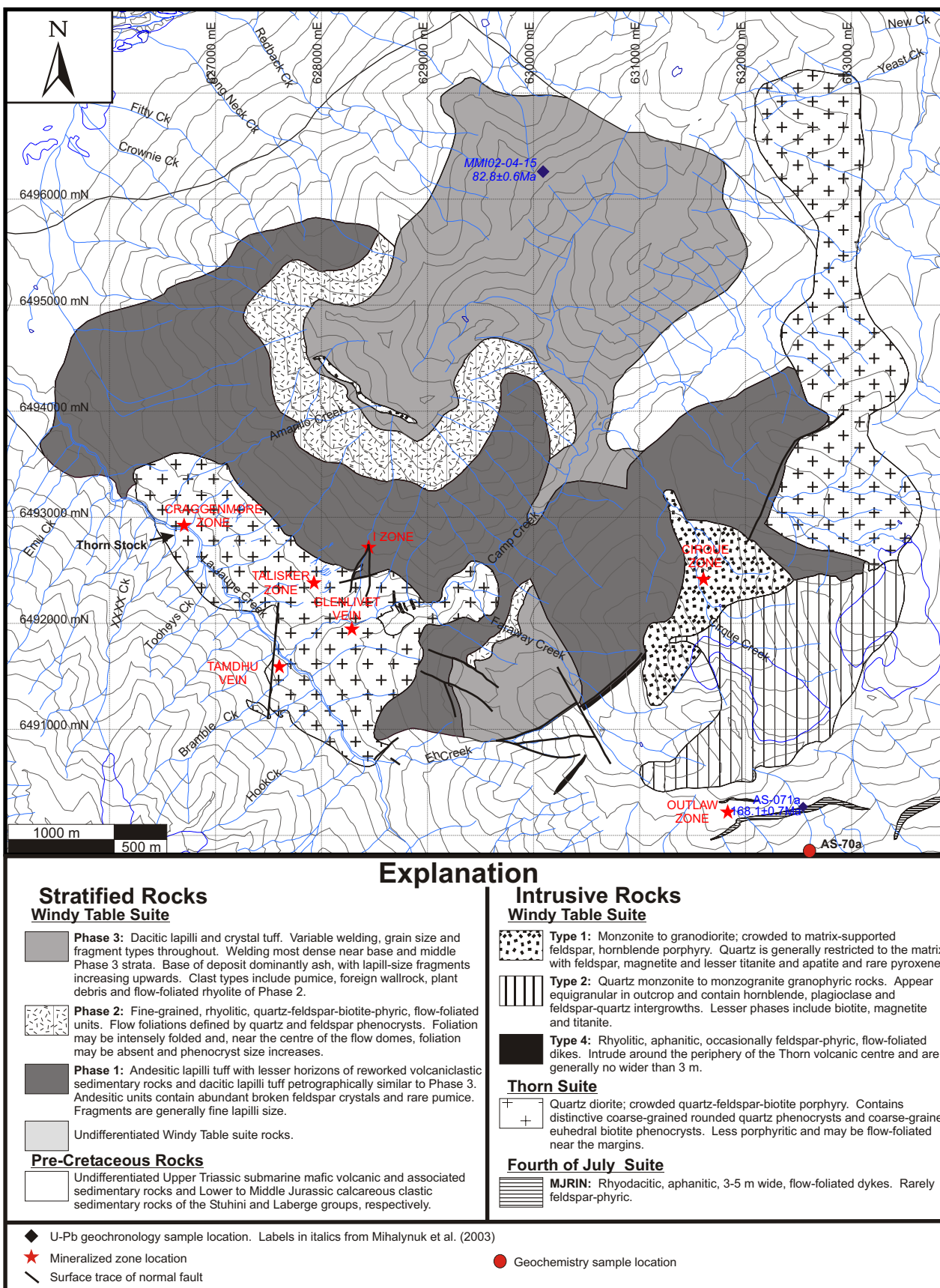● Geochemistry sample location

Figure 3. Geology of the Thorn property, showing locations of geochronology and geochemistry samples taken there.

property in the Little Trapper Lake area, an andesitic lapilli and crystal tuff, whose stratigraphic relation to Stuhini Group rocks on the Thorn property is not known, yielded a U-Pb SHRIMP-RG zircon age of 249 ±6.4 Ma (Table 2, sample 04AS-21; Fig 1, 4a), based on the weighted mean of the spot analyzes. Spots AS21-2, AS21-5 and AS-21-6 are interpreted to have undergone postcrystallization Pb loss and are not considered in the statistical analysis. No correlation was noted between older and younger ages to core and rims of zircon grains. It is unclear if this age represents Paleozoic basement rocks similar to those of the Wann River orthogneiss (Currie, 1990) or if it represents Stuhini Group rocks with a slightly older age than the accepted range for the group.

The Stuhini Group locally contains significant quantities of intrusive rocks, commonly associated with pyroclastic rocks correlative in age (*e.g.*, Willison Bay; Mihalynuk, 1999). South of the Thorn property in the Bing area near the Sheslay River, two U-Pb zircon ages on subvolcanic intrusive rocks were obtained using SHRIMP-RG as part of this study. A strongly foliated gabbro containing large plagioclase crystals (2–15 mm) and interstitial hornblende yielded a U-Pb SHRIMP-RG zircon age of 214.2 ±2.4 Ma (Table 2, sample 04AS-27; Fig 1, 4c). The zircons analyzed were extremely well behaved and did not yield multiple ages in spite of noted cores. Machine drift was encountered during this analysis, as seen in the weighted mean diagram, which shows a constantly decreasing age with each analysis. Spot AS27-5 is interpreted to have undergone postcrystallization Pb loss and was therefore not considered in the statistical analysis. Spots AS27-6 through 12 were used for statistical analysis because they form a more consistent weighted mean than spots AS27-1 though 4. Mihalynuk (1999) interpreted the foliated gabbroic rocks as subvolcanic intrusions. An equigranular granodiorite located approximately 5 km north of the foliated gabbro yielded a U-Pb SHRIMP-RG
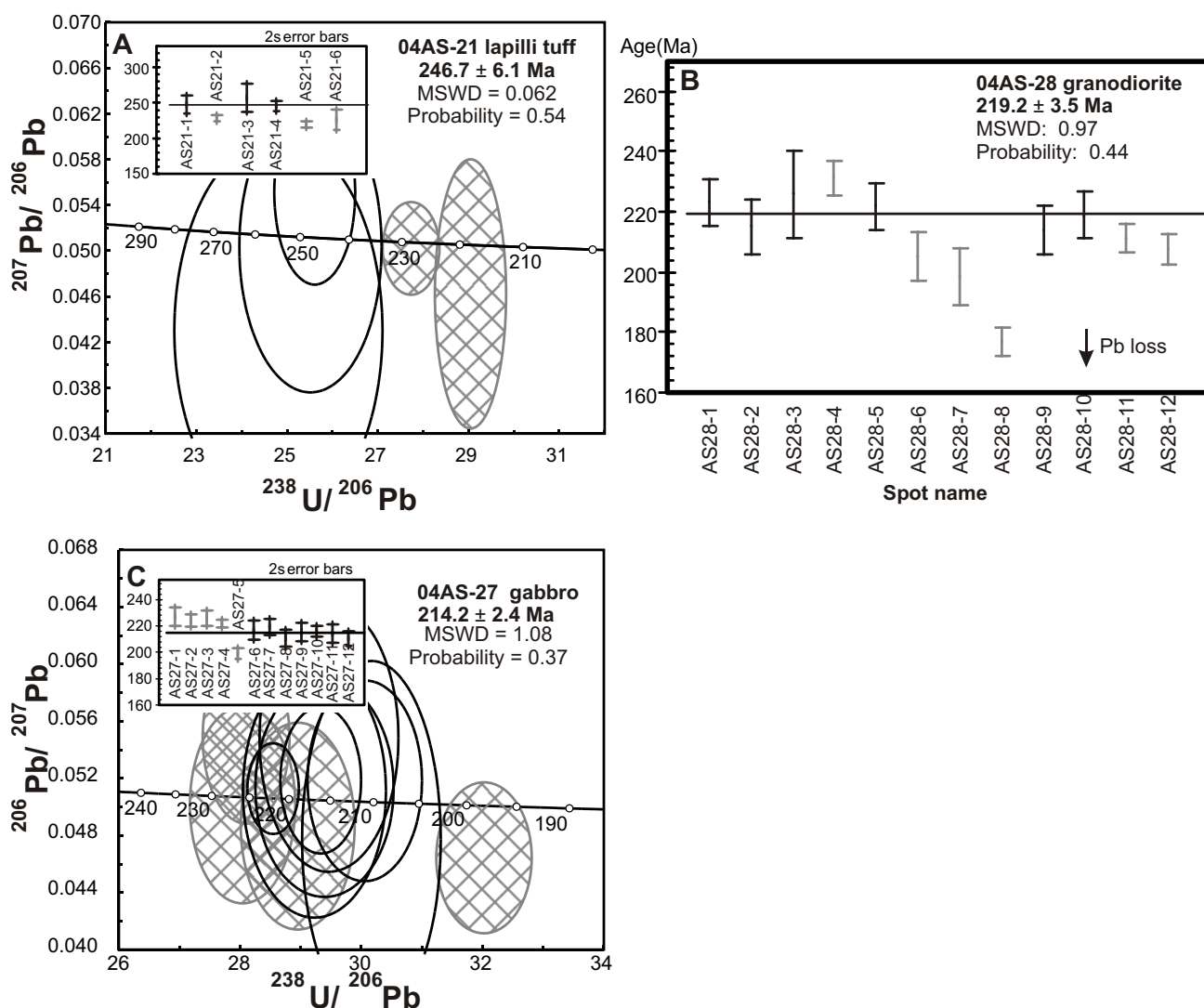

Figure 4. Weighted mean ^{206}Pb/^{238}U age plots for zircons from samples of intrusive and extrusive Stuhini Group rocks from the region surrounding the Thorn property. Ages are determined by weighted mean. Grey spot data are rejected due to either Pb loss or inheritance. Tera-Waserburg concordia plots are shown for comparison between concordia and weighted-mean ages. All errors are at 2σ levels. Tera-Waserburg plots are ^{207}Pb/^{206}Pb vs. ^{238}U/^{206}Pb. 'Point data' represent individual ablated and ionized points from separate zircons on a grain mount.

TABLE 2. SENSITIVE HIGH-RESOLUTION ION MICROPROBE – REVERSE GEOMETRY (SHRIMP-RG) U-PB ZIRCON ANALYTICAL DATA FOR SAMPLES OF STUHINI GROUP ROCKS FROM THE STUDY AREA.

Sample spot	$^{206}Pb^{1}$ (%)	U (ppm)	Th (ppm)	$\frac{^{232}Th}{^{238}U}$	$^{206}Pb^{2}$ (ppm)	$\frac{^{206}Pb^{2}}{^{238}U}$	1 (%)	$\frac{^{207}Pb}{^{206}Pb^{2}}$	1 (%)	Apparent age $^{206}Pb/^{238}U^{3}$	1 (Ma)
Unknown magmatic suite											
Sample 04-AS21 (andesitic lapilli tuff):											
AS21-1	-0.1	53	19	0.37	10.3	0.039089	2.51	0.0504	1.79	247.42	-6.34
AS21-2	0.09	921	308	0.35	3.3	0.035994	0.92	0.0502	28.48	227.76	-2.11
AS21-3	-1.04	28	12	0.47	16.1	0.040201	3.78	0.043	0.95	256.67	-9.82
AS21-4	0.5	151	104	0.71	6	0.038944	1.42	0.0551	5.05	245.07	-3.59
AS21-5	0.22	342	47	0.14	10.3	0.034581	1	0.0462	10.17	218.67	-2.26
AS21-6	-0.82	36	21	0.6	18.6	0.035379	3.01	0.0441	1.09	225.93	-7.1
Stuhini Group											
Sample 04-AS28 (granodiorite):											
AS28-1	-0.82	81	25	0.32	8.2	0.034867	1.71	0.044	2.42	222.73	-3.9
AS28-2	0.36	157	78	0.51	5.7	0.033951	2.16	0.0533	4.59	214.47	-4.66
AS28-3	0.09	53	15	0.3	11.4	0.035598	3.14	0.0514	1.62	225.28	-7.19
AS28-4	-0.22	181	83	0.47	6.2	0.036346	1.2	0.049	5.66	230.64	-2.86
AS28-5	-0.64	86	38	0.45	9.8	0.034686	1.74	0.0454	2.56	221.2	-4
AS28-6	-0.76	67	23	0.35	9.2	0.032001	1.91	0.0441	1.85	204.59	-4.01
AS28-7	-0.06	64	21	0.34	9.7	0.031169	2.32	0.0496	1.7	197.98	-4.69
AS28-8	0.12	105	33	0.32	6.2	0.027758	1.34	0.0505	2.51	176.3	-2.45
AS28-9	-0.73	84	22	0.27	8.4	0.033438	1.8	0.0445	2.4	213.56	-3.93
AS28-10	-0.17	132	69	0.54	6.3	0.034381	1.74	0.0491	3.91	218.28	-3.85
AS28-11	0.03	247	59	0.25	4.6	0.033255	1.05	0.0506	7.07	210.82	-2.28
AS28-12	0.03	181	41	0.24	5.4	0.032675	1.22	0.0505	5.09	207.2	-2.59
Sample 04-AS27 (gabbro):											
AS27-1	-0.54	144	40	0.29	4.41	0.035548	1.47	0.0399	13.8	226.37	-3.41
AS27-2	0.52	240	71	0.31	7.3	0.035465	1.05	0.0548	4.5	223.51	-2.43
AS27-3	-0.07	149	36	0.25	4.54	0.035564	1.28	0.0501	5.6	225.42	-2.96
AS27-4	0.09	722	125	0.18	21.67	0.034941	0.61	0.0513	2.5	221.21	-1.37
AS27-5	-0.45	356	67	0.19	9.54	0.031154	1.02	0.0465	4.6	198.65	-2.07
AS27-6	0.08	128	44	0.36	3.75	0.034126	1.65	0.0511	7.1	216.15	-3.66
AS27-7	-0.23	192	78	0.42	5.68	0.034425	1.33	0.0487	6.1	218.67	-2.99
AS27-8	0.33	195	96	0.51	5.57	0.033281	1.49	0.0477	10.7	210.36	-3.23
AS27-9	0.11	276	87	0.32	8.06	0.033933	1.59	0.0513	6.1	214.88	-3.47
AS27-10	0.18	420	236	0.58	12.26	0.034005	0.93	0.0519	4	215.19	-2.05
AS27-11	0.55	129	66	0.53	3.76	0.033849	1.59	0.0548	7	213.42	-3.51
AS27-12	0.19	161	55	0.35	4.6	0.033184	1.28	0.0518	5.5	210.06	-2.77

[1] common lead

[2] atomic ratios of radiogenic Pb

[3] $^{206}Pb/^{238}U$ age using ^{207}Pb to correct for common lead

zircon age of 219.2 ±3.5 Ma (Table 2, sample 04AS-28; Fig 1, 4b). Spots AS28-6, 7, 8, 11 and 12 are interpreted to have undergone postcrystallization Pb loss and were therefore not considered in the statistical analysis. Spot AS28-4 is interpreted as containing an inherited component, likely of Stuhini Group affinity, and was not considered in the statistical analysis. No correlation was noted between older and younger ages to crystal interiors and edges, respectively.

SINWA FORMATION

The upper part of the Stuhini Group contains the Sinwa Formation, which can be traced discontinuously throughout the study area (Souther, 1971; Fig 3). The Sinwa Formation ranges in thickness from 5 to 20 m and unconformably overlies Stuhini Group clastic sedimentary rocks on the Thorn property (Simmons, 2005).

It comprises two main rock types: lower limestone and upper clastic sedimentary rocks. Dolomitization, skarn development and recrystallization of limestone are widespread. Local boulder conglomerate units containing volcanic and intrusive rocks may correlate with the "Limestone Boulder Conglomerate" of Mihalynuk (1999), which separates Upper Triassic Stuhini Group strata from Pliensbachian argillite of the Laberge Group in the Moon Lake area, north of the study area.

Laberge Group

The Laberge Group is exposed over the entire length of the study area, extending from the vicinity of the Golden Bear mine in the south to the Yukon in the north (Fig 1). It is a major map unit in the study area. Souther (1971) estimated the thickness of the Laberge Group in the region to be 3100 m, although others have estimated it to be as much as 5000 m (*e.g.*, Bultman 1979). The Laberge Group comprises boulder to cobble conglomerate, immature sandstone and siltstone, wacke and argillite, all of which are generally calcareous. Correlation of individual sequences is difficult due to rapid lateral facies changes and lack of marker horizons. On the Thorn property, Laberge Group rocks overlie rocks of the Stuhini Group along a low-angle unconformably (Simmons *et al.,* 2005). These strata are thought to be an overlap assemblage linking terranes by the Early Jurassic (Wheeler *et al.*, 1991; Mihalynuk 1999).

Fourth of July Suite (Middle Jurassic)

Jurassic plutons are common in the Coast batholith to the northwest of the study area, where they in part form the Fourth of July plutonic suite of Mihalynuk (1999). They are sparsely observed southeast of the Taku River. During this study, several intrusions of the Fourth of July suite were recognized in one location on the Thorn property and dated at 168.1 ±0.7 Ma (Table 3, sample AS-071a; Fig 3, 5) by TIMS U-Pb zircon geochronology. Four fractions were analyzed and all yielded concordant analyses. Fractions A and B give somewhat older ages than fractions C and D. The best estimate for age of crystallization of the sample is given by the total range of $^{206}Pb/^{238}U$ ages for the concordant and overlapping fractions A and B. Fractions C and D are interpreted to have experienced postcrystallization Pb loss. Intrusions of this age on the Thorn property are 3 to 5 m wide, fine-grained, aphanitic rhyodacite dikes (Fig 3). The 168.1 ±0.7 Ma age from the rhyodacite dike is not a common age regionally for Jurassic magmatism. However, biotite cooling ages from the Fourth of July plutonic suite

can be as young as 164 Ma (*e.g.*, Roots and Parrish, 1988), which suggests the potential for plutonic rocks of similar age lying to the west of the study area. Fourth of July intrusions have important tectonic implications, as they apparently constrain the amalgamation and accretion of the Stikine, Cache Creek and Quesnel terranes.

Late Cretaceous Rocks

As the Late Cretaceous rocks will be discussed in more detail elsewhere (A.T. Simmons *et al.*, work in progress), these rocks are only briefly summarized here.

Following the accretion of the Stikine arc, a subduction zone was re-established west of the current location of Stikinia. Magmatism related to this subduction is recorded in three events at the Thorn property, beginning with the 93 to 88 Ma Thorn suite and followed by the 86 to 80 Ma Windy Table suite and the 58 to 54 Ma Sloko suite (Simmons, 2005). Together, the Thorn and Windy Table suites form the Late Cretaceous volcanoplutonic belt, which extends for at least 300 km from the Golden Bear mine to the BC-Yukon border (Simmons *et al.*, 2005).

Rocks of the Thorn suite are typified by the 'Thorn stock', which is a quartz-plagioclase-biotite-porphyritic quartz diorite. Large (>1 cm) euhedral biotite phenocrysts and rounded quartz phenocrysts are diagnostic of this rock type in the Late Cretaceous volcanoplutonic belt. The Windy Table suite is divided into intrusive and extrusive rocks. The extrusive rocks unconformably overlie the Thorn stock and cover the majority of the map area on the Thorn property (Simmons *et al.*, 2005). The volcanic strata form a volcanic sequence, greater than 5 km wide and 1600 m thick, that was deposited in a volcanic-tectonic depression. Rock types in the sequence include variably welded, dacitic to andesitic, crystal and lapilli tuffs with lesser volcaniclastic rocks and flow-foliated rhyolitic flow domes and shallow-level intrusions. Mihalynuk *et al.* (2003) reported a TIMS U-Pb zircon age of 82.8 ±0.6 Ma near the top the volcanic sequence. There are several varieties of subvolcanic intrusions in the Windy Table suite, including

TABLE 3. ISOTOPE DILUTION – THERMAL IONIZATION MASS SPECTROMETRY (ID-TIMS) U-PB ZIRCON ANALYTICAL DATA FOR SAMPLES FROM THE THORN PROPERTY.

Sample fraction[1]	Weight (mg)	U[2] (ppm)	Pb[3] (ppm)	$\frac{^{208}Pb^{[4]}}{^{204}Pb}$	Pb[5] (pg)	$^{208}Pb^{[3]}$ (%)	Isotopic ratios (error in % at 1σ level)[6]			Apparent age in Ma (error in % at 2σ level)[6]		
							$^{206}Pb/^{238}U$	$^{207}Pb/^{235}U$	$^{207}Pb/^{206}Pb$	$^{206}Pb/^{238}U$	$^{207}Pb/^{235}U$	$^{207}Pb/^{206}Pb$
Fourth of July suite												
Sample AS-071a (rhyodacite dyke):												
A	0.012	256	6.9	1406	4	11.8	0.02645 (0.14)	0.1807 (0.46)	0.04956 (0.41)	168.3 (0.5)	168.7 (1.4)	174 (19)
B	0.011	617	16.6	2372	5	11.7	0.02639 (0.12)	0.1799 (0.29)	0.04944 (0.22)	167.9 (0.4)	167.9 (0.9)	169 (10)
C	0.014	396	10.6	2632	3	12	0.02597 (0.11)	0.1770 (0.31)	0.04942 (0.26)	165.3 (0.4)	165.5 (1.0)	168 (12)
D	0.017	265	7	751	10	11.3	0.02598 (0.14)	0.1777 (0.44)	0.04960 (0.37)	165.3 (0.5)	166.1 (1.4)	176 (18)

[1] zircon fraction identifier

[2] U blank correction of 1 pg ±20%; U fractionation corrections measured for each run with a double ^{233}U-^{235}U spike (about 0.005/amu)

[3] radiogenic Pb

[4] measured ratio corrected for spike and Pb fractionation of 0.0037/amu ±20% (Daly collector), which was determined by repeated analysis of NBS Pb 981 standard

[5] total common Pb in analysis based on blank isotopic composition

[6] corrected for blank Pb, U and common Pb; common Pb corrections based on Stacey and Kramers (1975) model Pb at the age of the rock or the $^{207}Pb/^{206}Pb$ age of the rock
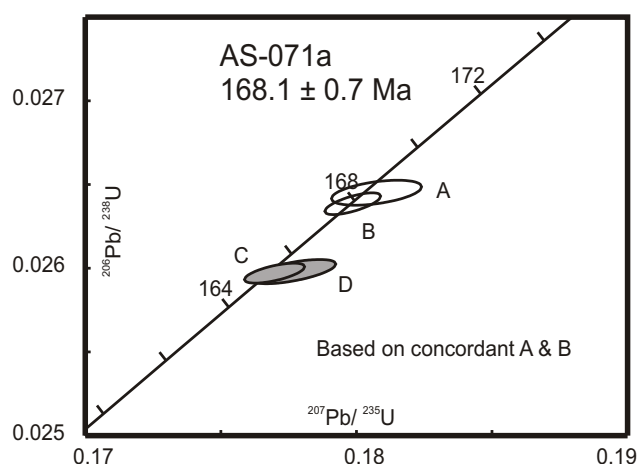
Figure 5. U-Pb concordia plot for a dike of the Fourth of July intrusive suite on the Thorn property. Zircon for this sample was analyzed by the isotope dilution – thermal ionization mass spectrometry (ID-TIMS) method. Empty ellipses and filled ellipses denote fractions used and rejected, respectively, for the age calculation.

variably porphyritic quartz monzonite to monzonite, plagioclase-megacrystic monzonite and flow-foliated rhyodacite dikes. These rocks are spatially, temporally and genetically related to veins at the Thorn property characterized by high-sulphidization mineral assemblages.

Sloko Suite Magmatism (58–54 Ma)

Souther (1971) mapped abundant early Tertiary, Sloko plutonic and volcanic rocks along the Late Cretaceous volcanoplutonic belt from the vicinity of the Golden Bear mine to the Tulsequah area. Between this study and that of Mihalynuk *et al.* (2003), only two locations are known where unequivocal Sloko plutonic rocks crop out. Both examples are plagioclase-biotite-porphyritic diorite in the Lisadele Lake area and the Sutl area, where they intrude into Laberge Group clastic sedimentary rocks. These rocks yielded SHRIMP U-Pb zircon ages of 56.3 ±0.7 Ma and

55.5 ±0.6 Ma, respectively (Fig 2, 6a, b; Table 4). For sample 04AS-11, no correlation was noted of older and younger ages to crystal interiors and edges, respectively. Spots 4AS11-1, 3, 5 and 12 are interpreted to have undergone postcrystallization Pb loss and were not considered in the statistical analysis. Spot 4AS11-2 is interpreted to contain an inherited component and was not considered in the statistical analysis. For sample 04AS-19, no correlation was noted of older and younger ages to crystal interiors and edges, respectively. Spots 4AS19-1, 2, 5 and 7 are interpreted to contain an inherited component and were not considered in the statistical analysis. The petrological similarity between this diorite and the Thorn stock makes it very difficult to unequivocally distinguish the two rock suites in the field. One criterion used was that Sloko suite rocks generally contain less quartz and are rarely unaltered.

GEOCHEMISTRY

Using major element geochemistry to classify rocks of the study area is problematic due to high degrees of acid leaching and alteration, which result in a net loss of CaO and Na_2O, and potential increases in K_2O, Al_2O_3 and SiO_2. Nonetheless, in order to build criteria for distinguishing these rocks from one another through varying degrees of alteration, representative rock units judged to be in their least altered states were analyzed. High degrees of variation in K_2O and Na_2O with respect to silica indicate that some of the major elements were, at least in part, mobile during postemplacement processes, such as alteration (*e.g.*, Fig 7c). However, trends that reflect fractionation processes are still present.

All rocks in this study are classified as relatively mafic units by the Zr/TiO_2 versus Nb/Y plot (Fig 7a). Stuhini Group rocks plot mainly as basaltic units, which is consistent with the known geochemistry of Stuhini Group volcanic rocks (*e.g.*, Mihalynuk, 1999). Two of the Stuhini Group rocks plot as 'andesite/basalt'; both of these rocks are interpreted as subvolcanic Stuhini Group intrusions, one being a cumulate gabbroic rock and the other a quartz monzonite to granodiorite. Although there is a paucity of
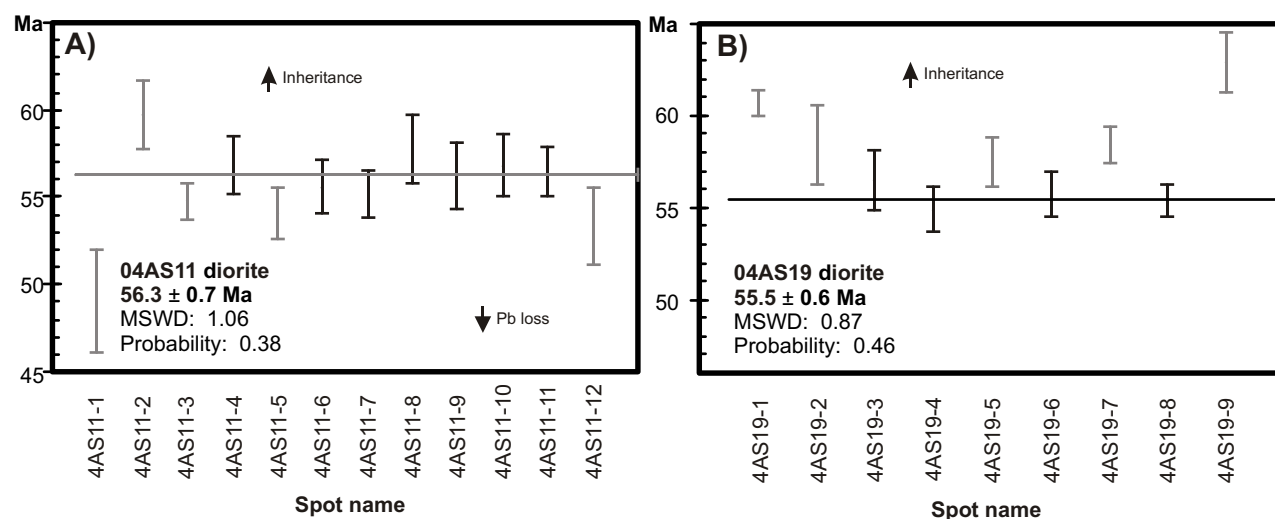

Figure 6. Weighted mean $^{206}Pb/^{238}U$ age plots for zircons from samples of intrusive rocks of the Sloko suite from the study area. Ages are determined by weighted mean. Grey spot data are rejected due to either Pb loss or inheritance. All errors are at 2σ levels. 'Point data' represent individual ablated and ionized points from separate zircons on a grain mount.

TABLE 4. SENSITIVE HIGH-RESOLUTION ION MICROPROBE – REVERSE GEOMETRY (SHRIMP-RG) U-PB ZIRCON ANALYTICAL DATA FOR SAMPLES OF SLOKO GROUP ROCKS FROM THE STUDY AREA.

Sample spot	$^{206}Pb^{1}$ (%)	U (ppm)	Th (ppm)	$\frac{^{232}Th}{^{238}U}$	$^{206}Pb^{2}$ (ppm)	$\frac{^{206}Pb^{2}}{^{238}U}$	1 (%)	$\frac{^{207}Pb}{^{206}Pb^{2}}$	1 (%)	Apparent age $^{206}Pb/^{238}U^{3}$	1 (Ma)
Sloko suite											
Sample 04AS11 (diorite porphyry):											
4AS11-1	0.4	265	80	0.31	1.74	0.00753	3.1	0.037	20	49	-1.5
4AS11-2	0.47	206	67	0.34	1.66	0.00954	1.6	0.0675	5.7	59.64	-0.97
4AS11-3	0.15	658	360	0.56	4.82	0.008461	1	0.0422	7	54.65	-0.54
4AS11-4	0	587	236	0.42	4.44	0.00887	1.5	0.0497	6.2	56.72	-0.83
4AS11-5	0.58	319	123	0.4	2.31	0.00827	1.4	0.0341	12.7	53.94	-0.75
4AS11-6	0	289	106	0.38	2.15	0.00863	1.9	0.046	23.7	55.48	-0.77
4AS11-7	0.28	394	127	0.33	2.91	0.00851	1.3	0.0397	11.1	55.11	-0.67
4AS11-8	0.5	183	59	0.33	1.42	0.00881	2	0.0325	30.3	57.61	-0.98
4AS11-9	0	183	47	0.26	1.37	0.00864	2	0.0381	25.6	56.1	-0.95
4AS11-10	0.25	525	175	0.34	4	0.00886	1.5	0.0491	3.7	56.71	-0.88
4AS11-11	0.16	366	98	0.28	2.77	0.00878	1.3	0.0475	8.4	56.32	-0.7
4AS11-12	0	339	124	0.38	2.41	0.00819	2.2	0.0376	19.7	53.2	-1.1
Sample 04AS19 (diorite porphyry):											
4AS19-1	0.04	1053	410	0.4	8.56	0.009515	0.65	0.0518	5.7	60.69	-0.35
4AS19-2	0.72	131	52	0.41	1.03	0.00936	2.3	0.0683	18.5	58.4	-1.1
4AS19-3	0.78	219	69	0.32	1.67	0.00881	1.5	0.0476	10.5	56.49	-0.84
4AS19-4	0.53	312	151	0.5	2.31	0.00844	1.2	0.0365	16.7	54.89	-0.6
4AS19-5	0.29	283	84	0.31	2.19	0.009084	1.1	0.0578	6.2	57.51	-0.67
4AS19-6	1.04	313	143	0.47	2.36	0.00841	1.9	0.0216	62.9	55.72	-0.63
4AS19-7	0	464	262	0.58	3.63	0.009021	0.9	0.0403	9.1	58.4	-0.51
4AS19-8	0.05	679	230	0.35	5.04	0.008504	0.72	0.0355	7.3	55.39	-0.41
4AS19-9	1.01	239	80	0.35	2.03	0.00996	1.3	0.0602	6.7	62.87	-0.81

[1] common lead

[2] atomic ratios of radiogenic Pb

[3] $^{206}Pb/^{238}U$ age using ^{207}Pb to correct for common lead

data, intrusive rocks of the Sloko and Fourth of July suites plot as 'andesite/basalt'. These compositions are not surprising, given that the Sloko suite rock sampled is a coarse-grained diorite porphyry. However, this is somewhat surprising for the rocks of the Fourth of July suite, which are fine-grained flow-foliated rhyolitic dikes. The high SiO_2 concentration of this rock type suggests it was a late-stage intrusive rock that may have partially crystallized in vapour phase; this relatively evolved state may explain the differences in trace element concentrations (Fig 7a, b). All rocks are classified as medium-K calcalkaline series, with the exception of one sample from the Stuhini Group, a subvolcanic quartz monzonite to granodiorite intrusion, which plots in the high-K field (Fig 7b). Importantly, Stuhini Group basaltic rocks plot in medium-K field, which is key distinction from Stuhini Group basaltic rocks farther north in the Tagish Lake area, where Mihalynuk (1999) showed Stuhini Group basaltic rocks to be significantly K rich, plotting as absarokite. There is no known explanation for this difference along strike in the arc.

The Ba/La ratios of all magmatic rocks from the study area exceed 20 (Fig 7d), suggestive of an arc rather than a back-arc setting (*e.g.*, Sasso and Clark, 1998; Bissig *et al.*, 2003). This environment is supported by the tectonic discrimination plots, which show that all samples plot as volcanic-arc granite (Fig 7e).

Stuhini Group and Fourth of July suite rocks also have relatively flat rare earth element (REE) patterns, the latter suite having higher overall concentrations of all REE and a negative Eu anomaly (Fig 7f). The Stuhini Group sample (Table 5, AS-070a; Fig 7f) is from a subaqueous massive basaltic flow, which typically yields flat, relatively enriched REE patterns indicative of partial melting of the upper mantle. Mihalynuk (1999) suggested that Fourth of July suite magmas display similar chemistry to mature volcanic arcs (Fig 7f); sample AS-071a does not display similar chemistry. The high SiO_2 concentration of this rock suggests that it was a late-stage intrusive rock; this relatively evolved state may explain the differences in REE concentrations. Sloko suite intrusive rocks are geochemically distinct from Stuhini Group and Fourth of July suite rocks, having steeper REE patterns (Fig 7f).

DISCUSSION AND CONCLUSIONS

Stuhini Group rocks represent a major geological unit within the Stikine Terrane, yet very little is known about origin, timing and chemistry of these rocks, mainly due to a lack of significant studies in these rocks. Data presented herein are meant to add to the existing data publicly available in the hope that a significant dataset can be put together to unravel the mysteries of Stuhini Group magmatism. Mapping during this study is consistent with previous ideas that the Stuhini Group records a dynamic environment interpreted as two major arc-building events (*e.g.*, Wheeler, 1961; Hart and Pelletier, 1989; Mihalynuk, 1999). Mihalynuk (1999) noted that evidence for the lower arc is observed at particular faults, in basal upper-arc conglomerate and as screens within late-arc subvolcanic Stuhini Group intrusions. Sample 04AS-21, taken south of the
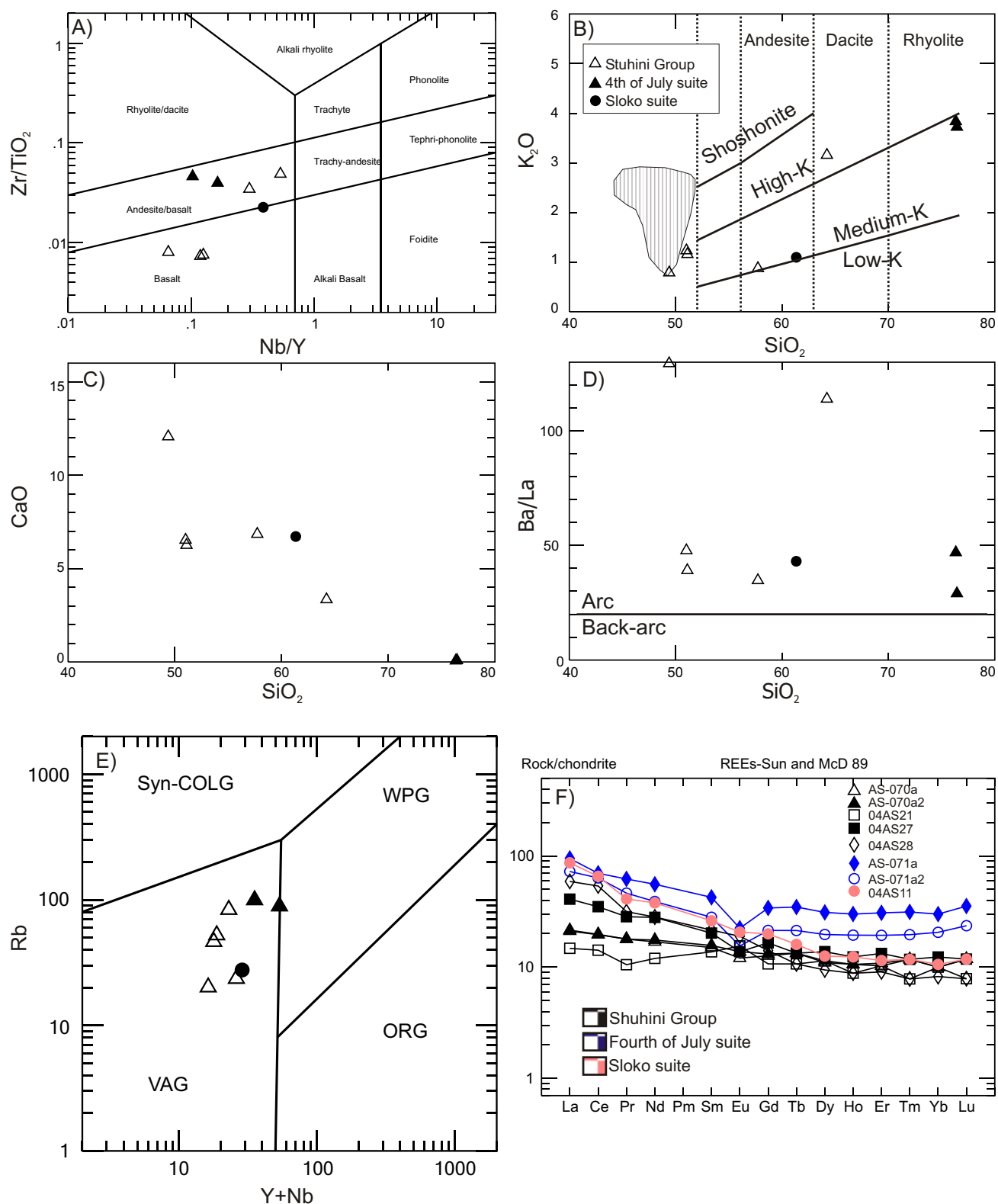
Figure 7. Various geochemical discrimination plots using major, trace and rare earth elements: A) Zr/TiO$_2$ versus Nb/Y *from* revised Winchester and Floyd (1977); *from* Pearce (1996); B) K$_2$O versus SiO$_2$ (*after* Gill, 1981); shaded area represents field for data collected by Mihalynuk (1999); C) CaO versus SiO$_2$ to show variation in major elements with minor changes in SiO$_2$; D) Ba/La versus SiO$_2$ for discrimination between arc and back-arc environments; E) Rb versus Y+Nb tectonic discrimination plot (*after* Pearce *et al.*, 1984); F) REE spider plot (*after* Sun and McDonough, 1989). Abbreviations: syn-COLG, syn-collisional granite; WPG, within-plate granite; VAG, volcanic arc granite; ORG, ocean ridge granite.

TABLE 5. GEOCHEMICAL DATA FOR ALL ROCKS IN THIS STUDY.

Parameter		Stuhini Group					Fouth of July suite		Sloko intrusive rocks
	Sample:	AS070a	AS070a2	04AS27	04AS28	04AS21	AS071	AS071	04AS11
SiO$_2$	wt%	47.31	47.21	56.8	63.5	49.4	73.55	73.68	58.1
TiO$_2$	wt%	0.94	0.93	0.79	0.45	0.76	0.51	0.56	0.6
Al$_2$O$_3$	wt%	17.58	17.6	18.7	17.85	15.64	14.75	14.9	16.35
Fe$_2$O$_3$	wt%	10.56	10.43	4.24	3.74	12.12	2.55	2.5	5.69
FeO	wt%	6.29	6.21	2.52	2.23	------	2.12	1.61	5.66
MnO	wt%	0.17	0.16	0.06	0.07	0.18	0.03	0.02	0.12
MgO	wt%	4.71	4.61	3.43	0.88	8.71	0.93	0.89	2.54
CaO	wt%	5.79	6.04	6.73	3.3	12.06	0.08	0.06	6.36
Cr$_2$O$_3$	wt%	0.02	0.02	0.01	0.01	0.07	0.02	0.01	------
Na$_2$O	wt%	4.15	4.12	6.29	5.56	0.03	0.09	0.06	3.26
K$_2$O	wt%	1.07	1.14	0.86	3.12	0.79	3.58	3.7	1.04
BaO	wt%	0.04	0.04	0.04	0.15	0.05	0.08	0.1	0.08
P$_2$O$_5$	wt%	0.19	0.19	0.33	0.15	0.18	0.04	0.03	0.21
LOI	wt%	7.01	6.89	1.53	1.73	12.25	2.97	2.79	4.73
Total	wt%	*99.58*	*99.41*	*99.9*	*100.5*	*100*	*99.19*	*99.29*	*99.4*
Ba	ppm	199.5	239	337	1595	453	653	807	888
Co	ppm	33.5	32.5	11.5	8.7	49.2	3.7	3.8	14.6
Cr	ppm	120	120	60	100	510	190	110	50
Cs	ppm	12.7	17.5	1.2	2.6	1.8	12.1	5.9	2
Cu	ppm	132	132	47	15	130	6	------	18
Ga	ppm	16	16	22	23	17	16	17	21
Hf	ppm	2	1	5	3	1	5	4	2
Mo	ppm	------	------	2	3	1	2	4	4
Nb	ppm	2	2	6	8	1	5	5	8
Ni	ppm	33	33	19	12	85	12	11	11
Pb	ppm	5	7	16	9	2.5	6	6	12
Rb	ppm	46.3	52.2	23.5	83.4	20.1	88.8	99.4	27.6
Sn	ppm	1	1	2	1	1	2	2	1
Sr	ppm	529	538	896	818	209	34.6	35.4	871
Ta	ppm	------	------	0.5	------	0.25	------	------	0.6
Th	ppm	1	1	4	4	0.5	4	4	8
Tl	ppm	------	------	------	------	0.25	0.5	0.6	------
U	ppm	0.7	0.6	2	1.7	0.25	1.1	1.1	4.3
V	ppm	366	353	201	80	329	50	54	146
W	ppm	1	1	4	2	8	1	2	2
Y	ppm	15.9	16.8	20.1	15	15.3	48.5	30.4	20.7
Zn	ppm	74	72	46	46	108	34	31	81
Zr	ppm	45.9	44.1	166	133	36.7	146.5	138	86.1
La	ppm	5.1	5	9.7	14	3.5	22.5	17.2	20.6
Ce	ppm	12.1	12	21.4	32.9	8.7	42.8	38.9	40.2
Pr	ppm	1.7	1.7	2.7	3	1	5.9	4.4	3.9
Nd	ppm	7.9	8.2	13.1	13.2	5.6	26	18.2	17.7
Sm	ppm	2.3	2.4	3.1	3.3	2.1	6.5	4.3	4
Eu	ppm	0.7	0.8	0.8	1.1	0.9	1.3	0.9	1.2
Gd	ppm	2.6	2.7	3.4	2.9	2.2	7	4.4	4.1
Tb	ppm	0.5	0.5	0.5	0.4	0.4	1.3	0.8	0.6
Dy	ppm	2.8	2.9	3.5	2.4	2.9	7.9	5	3.2
Ho	ppm	0.6	0.6	0.7	0.5	0.5	1.7	1.1	0.7
Er	ppm	1.7	1.8	2.2	1.5	1.7	5.1	3.2	1.9
Tm	ppm	0.3	0.3	0.3	0.2	0.2	0.8	0.5	0.3
Yb	ppm	1.7	1.7	2.1	1.4	1.7	5.1	3.5	1.8
Lu	ppm	0.3	0.3	0.3	0.2	0.2	0.9	0.6	0.3

Major oxide concentrations from XRF; all others by ICP-MS, from ALS Chemex, North Vancouver, BC

Thorn property in the Little Trapper Lake area, is an andesite lapilli tuff that was previously mapped as Stuhini Group and yielded an age of 249 ±6.4 Ma. This rock, although poorly stratigraphically constrained, may represent the earliest known volcanism related to early arc-building processes of the Stuhini Group. Alternatively, it may simply represent a previously unrecognized period of arc building. Magmatism during the late arc-building process

is recorded in samples 04AS-27 and 04AS-28, which yielded ages of 214.2 ±2.4 and 219.2 ±3.5 Ma, respectively. Both of these rocks are interpreted to be subvolcanic intrusive rocks related to late Stuhini Group volcanism. The geochemistry of Stuhini Group rocks from this study is somewhat distinct from those of previous studies to the north, for reasons that are presently unknown. Nonetheless, data from the study area are similar to those from rocks that reflect arc magmatism.

Other magmatic rocks of non-Cretaceous age in the study area include intrusive rocks of the Fourth of July and Sloko suites. Fourth of July suite rocks are spatially very limited and occur as very narrow dikes. These dikes crosscut the upper stratigraphy of the Stuhini Group, as well as the clastic sedimentary rocks of the Lower to Middle Jurassic Laberge Group. Temporally, these rocks are slightly younger than those described in the Tagish Lake area, where the Fourth of July suite rocks intrude overlap assemblages and record the timing of amalgamation of the Stikine, Cache Creek and Quesnel terranes. Sloko suite rocks are distributed throughout the study area, with abundance increasing towards the west. These rocks represent a continental arc built in the earliest Eocene. Insufficient data are presently available to adequately characterize these rocks.

REFERENCES

Bacon, C.R., Persing, J.M., Wooden, J.L. and Ireland, R.R. (2000): Late Pleistocene granodiorite beneath Crater Lake Caldera, Oregon, dated by ion microprobe; *Geology*, volume 28, pages 467–470.

Baker, D.E.L. (2003): 2003 geological, geochemical and diamond drilling report on the Thorn property; *BC Ministry of Energy, Mines and Petroleum Resources*, Assessment Report 27120.

Bissig, T., Clark, A.H., Lee, J.K.W. and von Quadt, A. (2003): Petrogenetic and metallogenic responses to Miocene slab flattening: new constraints from El Indio – Pascua Au-Ag-Cu belt, Chile/Argentina; *Mineralium Deposita*, volume 38, pages 844–862.

Bultman, T.R. (1979): Geology and tectonic history of the Whitehorse Trough west of Atlin; unpublished PhD thesis, *Yale University*, 284 pages.

Cumming, G.L. and Richards, J.R. (1975): Ore lead isotope ratios in a continuously changing Earth; *Earth and Planetary Science Letters*, volume 63, pages 155–171.

Currie, L.D. (1990): Metamorphic rocks in the Florence Range, Coast Mountains, northwestern British Columbia (104M/8); *in* Geological Fieldwork 1989, *BC Ministry of Energy, Mines and Petroleum Resources*, Paper 1990-1, pages 197–203.

Gabrielse, H. (1969): Geology of the Jennings River map-area, British Columbia (104-O); *Geological Survey of Canada*, Paper 68-55, 37 pages.

Gill, J.B. (1981): Orogenic andesites and plate tectonics; *Springer-Verlag*, 390 pages.

Hart, C.J.R. (1995): Magmatic and tectonic evolution of the Intermontane Superterrane and the Coast Plutonic Complex in southern Yukon Territory; unpublished MSc thesis, *University of British Columbia*, Vancouver, BC, 198 pages.

Hart, C.J.R. and Pelletier, K.S. (1989): Geology of Carcross (105D/2) and part of Robinson (105D/7) map areas; *Indian and Northern Affairs Canada*, Open File 1989-1, 84 pages.

Hart, C.J.R., Pelletier, K.S., Hunt, J. and Fingland, M. (1989): Geological map of Carcross (105D/2) and part of Robinson

(105D/7) map areas; *Indian and Northern Affairs Canada*, Open File Map 1989-1.

Ireland, T.R. and Williams, I.S. (2003): Considerations in zircon geochronology by SIMS; *Reviews in Mineralogy and Geochemistry*, volume 53, pages 215–241.

Jackson, J.L. (1992): Tectonic analysis of the Nisling, northern Stikine and northern Cache Creek Terranes, Yukon and British Columbia; unpublished PhD thesis, *University of Arizona*, 200 pages.

Kerr, F.A. (1948): Taku River map area, British Columbia; *Geological Survey of Canada*, Memoir 248.

Krogh, T.E (1982): Improved accuracy of U-Pb zircon ages by the creation of more concordant systems using an air abrasion technique; *Geochimica et Cosmochimica Acta*, volume 46, pages 637–649.

Logan, J.M., Drobe, J.R. and McClelland, W.C. (2000): Geology of the Forrest Kerr – Mess Creek area, northwestern British Columbia (NTS 104B/10, 15 and 104G/2 and 7W), *BC Ministry of Energy Mines and Petroleum Resources*, Bulletin 104, 164 pages.

Ludwig, K.R. (1980): Calculation of uncertainties of U-Pb isotopic data; *Earth and Planetary Science Letters*, volume 46, pages 212–220.

Ludwig, K.R. (1999): ISOPLOT: a plotting ad regression program for radiogenic-isotope data; *United States Geological Survey*, Open File 91-445, 41 pages.

Ludwig, K.R. (2001): SQUID 1.00, a users manual; Berkeley Geochronology Center, Special Publication 2, 17 pages.

Ludwig, K.R. (2003): ISOPLOT 3.00: a geochronological toolkit for Microsoft Excel; *Berkeley Geochronology Centre*, Special Publication 4.

Mihalynuk, M.G. (1999): Geology and mineral resources of the Tagish Lake area, BC; *BC Ministry of Energy, Mines and Petroleum Resources*, Bulletin 105.

Mihalynuk, M.G., Gabites, J.E., Orchard, M.J. and Tozer, E.T. (1997): Age of the Willison Bay pluton and overlying sediments: implications for the Carnian stage boundary; *in* Geological Fieldwork 1996, *BC Ministry of Energy, Mines and Petroleum Resources*, Paper 1997-1, pages 171–179.

Mihalynuk, M.G., Mortensen, J., Friedman, R., Panteleyev, A. and Awmack, H.J. (2003): Cangold partnership: regional geologic setting and geochronology of high-sulphidation mineralization at the Thorn property, British Columbia; *BC Ministry of Energy, Mines and Petroleum Resources*, GeoFile 2003-10.

Mihalynuk, M.G., Nelson, J. and Diakow, L. (1994): Cache Creek Terrane entrapment: oroclinal paradox within the Canadian Cordillera; *Tectonics*, volume 13, pages 575–595.

Mihalynuk M.G. and Smith, M.T. (1992): Highlights of 1991 mapping in the Atlin-west map area (104N/12); *in* Geological Fieldwork 1991, *BC Ministry of Energy Mines and Petroleum Resources*, Paper 1992-1, pages 221–227.

Monger, J.W.H. (1984): Cordilleran tectonics: a Canadian perspective; *Bulletin de la Société Géologique de France*, series 7, volume 26, pages 197–324.

Monger, J.W.H., Wheeler, J.O., Tipper, H.W., Gabrielse, H., Harms, T., Struik, L.C., Campbell, R.B., Dodds, C.J., Gehrels, G.E. and O'Brien, J. (1991): Cordilleran terranes; *in* Geology of the Cordilleran Orogen in Canada, Gabrielse, H. and Yorath, C.J., Editors, *Geological Survey of Canada*, Geology of Canada, volume 4, pages 281–327.

Nelson, J.L. (1993): The Sylvester Allochthon: Upper Paleozoic marginal-basin and island-arc terranes in northern British Columbia; *Canadian Journal of Earth Sciences*, volume 30, pages 631–643.

Nixon, G.T., Archibald, D.A. and Heaman, L.M. (1993): [40]Ar-[39]Ar and U-Pb geochronometry of the Polaris Alaskan-type complex, British Columbia: precise timing of Quesnellia –

North America interaction; *Geological Association of Canada – Mineralogical Society of Canada*, Joint Annual Meeting, Program and Abstracts, page A76.

Parrish, R., Roddick, J.C., Loveridge, W.D. and Sullivan, R.W. (1987): Uranium-lead analytical techniques at the geochronology laboratory, Geological Survey of Canada; *in* Radiogenic Age and Isotopic Studies: Report 1, *Geological Survey of Canada*, Paper 87-2, pages 3–7.

Pearce, J.A. (1996): A users guide to basalt discrimination diagrams; *in* Trace element Geochemistry of Volcanic Rocks: Applications for Massive Sulphide Exploration, *Geological Association of Canada*, Short Course Notes, volume 12, pages 79-113.

Pearce, J.A., Harris, N.B.W. and Tindle, A.G. (1984): Trace element discrimination diagrams for the tectonic interpretation of granitic rocks; *Journal of Petrology*, volume 25, pages 956-983.

Ricketts, D.B., Evenchick, C.A., Anderson, R.G. and Murphy D.C. (1992): Bowser Basin, northern British Columbia: constraints on the initial timing of subsidence and Stikinia – North America interactions; *Geology*, volume 20, pages 1119–1122.

Roddick, J.C. (1987): Generalized numerical error analysis with application to geochronology and thermodynamics; *Geochimica et Cosmochimica Acta*, volume 51, pages 2129–2135.

Roots, C.F. and Parrish, R. R., 1988, Age of the Mount Harper volcanic complex, southern Ogilvie Mountains, Yukon; *in* Radiogenic Age and Isotopic Studies: Report 2, *Geological Survey of Canada*, Paper 88-2, pages 29–36.

Sasso, A.M. and Clark, A.H. (1998): The Farallón Negro Group, northwest Argentina: magmatic hydrothermal and tectonic evolution and implications for Cu-Au metallogeny in the Andean back-arc; *Society of Economic Geology Newsletters*, volume 34, pages 18–18.

Simmons, A.T. (2005): Geological and geochronological framework and mineralization characterization of the Thorn property, and associated volcanoplutonic complexes of northwestern British Columbia, Canada; unpublished MSc thesis, *University of British Columbia*, Vancouver, BC, 168 pages.

Simmons, A.T., Tosdal, R.M., Baker, D.E.L., Friedman, R.M. and Ullrich, T.D. (2005): Late Cretaceous volcano-plutonic arcs in northwestern British Columbia: implications for porphyry and epithermal deposits; *in* Geological Fieldwork 2004, *BC Ministry of Energy Mines and Petroleum Resources*, Paper 2005-1, pages 347–360.

Souther, J.G. (1971): Geology and mineral deposits of the Tulsequah map-area, British Columbia; *Geological Survey of Canada*, Memoir 362, 84 pages.

Stacey, J.S. and Kramers, J.D. (1975): Approximation of terrestrial lead evolution by a two-stage model; *Earth and Planetary Science Letters*, volume 26, pages 207-221.

Sun, S.S. and McDonough, W.F. (1989): Chemical and isotopic systematics of oceanic basalts: implications for mantle composition and processes; *in* Magmatism in the Ocean Basins, *Geological Society of London*, Special Publication 42, pages 313–345.

Thirlwall, M.F. (2000): Inter-laboratory and other errors in Pb isotope analyses investigated using a ^{207}Pb-^{204}Pb double spike; *Chemical Geology*, volume 163, pages 299–322.

Thorstad, L.E. and Gabrielse, H. (1986): The Upper Triassic Kutcho Formation, Cassiar Mountains, north-central British Columbia; *Geological Survey of Canada*, Paper 86-16, 53 pages.

Wheeler, J.O. (1961): Whitehorse map-area, Yukon Territory (105D); *Geological Survey of Canada*, Memoir 312, 156 pages.

Wheeler, J.O., Brookfield, A.J., Gabrielse, H., Monger, J.W.H., Tipper, H.W. and Woodsworth, G.J. (1991): Terrane map of the Canadian Cordillera; *Geological Survey of Canada*, Map 1713A, scale 1:2 000 000.

Wheeler, J.O. and McFeely, P. (1987): Tectonic assemblage map of the Canadian Cordillera; *Geological Survey of Canada*, Open File 1565.

Williams, I.S. (1998): U-Th-Pb geochronology by ion microprobe; *in* Applications of Micro Analytical Techniques to Understanding Mineralizing Processes, Volume 7, McKibben, M.A., Shanks, W.C., III and Ridley, W.I., Editors, *Reviews in Economic Geology*, pages 1–35.

Winchester, J.A. and Floyd, P.A. (1977): Geochemical discrimination of different magma series and their differentiation products using immobile elements; *Chemical Geology*, volume 20, pages 325–343.